JOURNAL OF GEOPHYSICAL RESEARCH, VOL. 105, NO. D24, PAGES 29,693–29,702, DECEMBER 27, 2000

A new lightning return stroke model based on antenna theory

Rouzbeh Moini,[1] Behzad Kordi,[2,1] Gholamreza Z. Rafi,[3,1] and Vladimir A. Rakov[4]

Abstract. A new approach based on antenna theory is presented to describe the lightning return-stroke process. The lightning channel is approximated by a straight and vertical monopole antenna with distributed resistance (a so-called lossy antenna) above a perfectly conducting ground. The antenna is fed at its lower end by a voltage source such that the antenna input current, which represents the lightning return-stroke current at the lightning channel base, can be specified. An electric field integral equation (EFIE) in the time domain is employed to describe the electromagnetic behavior of this lossy monopole antenna. The numerical solution of EFIE by the method of moments (MOM) provides the time-space distribution of the current and line charge density along the antenna. This new antenna-theory (or electromagnetic) model with specified current at the channel base requires only two adjustable parameters: the return-stroke propagation speed for a nonresistive channel and the channel resistance per unit length, each assumed to be constant (independent of time and height). The new model is compared to four of the most commonly used "engineering" return-stroke models in terms of the temporal-spatial distribution of channel current, the line charge density distribution, and the predicted electromagnetic fields at different distances. A reasonably good agreement is found with the modified transmission line model with linear current decay with height (MTLL) and with the Diendorfer-Uman (DU) model.

1. Introduction

The expression "lightning return-stroke model" is generally used to describe a specification of the time- and height-dependent current in the return-stroke channel to make possible the calculation of resultant remote electromagnetic fields [*Rakov and Uman*, 1998]. Most of the return-stroke models specify an analytical relation between the current at each point of the channel and the channel-base (ground level) current. Such an analytical relation also describes the propagation of the current wave along the channel. A suitable model should be characterized by a minimum number of adjustable parameters and be consistent with the measured characteristics of the return stroke, including (1) current at the base of the channel, (2) variation of light intensity with height, (3) upward propagation speed of the luminosity front, and (4) electromagnetic fields at various distances from the channel.

A discussion and comparison of the most common return-stroke models is found in the works of *Nucci et al.* [1990], *Thottappillil and Uman* [1993], *Thottappillil et al.* [1997], and *Rakov and Uman* [1998]. In this paper a new model of the lightning return stroke, an antenna-theory (AT) model, is presented and compared to the transmission line model (TL), the modified transmission line model with linear current decay with height (MTLL), the modified transmission line model with exponential current decay with height (MTLE), and the Diendorfer-Uman model (DU).

In the TL model the current injected at the channel base propagates upward without either distortion or attenuation as it would on a lossless transmission line but at the speed arbitrarily set at a value lower than the speed of light [e.g., *Uman and McLain*, 1969]. The channel is assumed to be initially uncharged, and the charge density along the channel becomes everywhere zero after the wave has traversed the channel. Because of this feature of the model, the fields calculated using the TL model are not consistent with measurements at later times and closer ranges [*Nucci et al.*, 1990; *Thottappillil et al.*, 1997].

In the MTLL model the current wave suffers no distortion but its amplitude decays linearly with height [e.g., *Rakov and Dulzon*, 1987]. The MTLE model is similar, but the current amplitude decays exponentially with height [e.g., *Nucci et al.*, 1990]. The final line charge density in the MTLL model is assumed to be the same at all heights, while in the MTLE model, it rapidly decreases with increasing height. Because of the charge density distribution in the MTLE model being unrealistically skewed toward the bottom of the channel, this model is not able to predict adequately the very close electric field [e.g., *Thottappillil et al.*, 1997]. In the case of MTLL model, the calculated fields are consistent with the measurements at all ranges [e.g., *Rakov and Dulzon*, 1991; *Thottappillil et al.*, 1997]. In the modified transmission line models (MTLL and MTLE), the current attenuation is specified arbitrarily while the shape of current waveform remains the same; that is, there is no dispersion.

The DU model and its modifications consider the channel current as the sum of two components, one due to a fast discharge of the leader channel core and the other due to a slower discharge of the corona sheath surrounding the channel core [e.g., *Diendorfer and Uman*, 1990]. These current components are assumed to be generated at the upward moving return-stroke front and to propagate downward. In the DU model, the distribution of line charge density along the channel during the return-stroke process is influenced by the inherent assumption that the current reflection coefficient at ground is equal to zero [e.g., *Thottappillil*

[1]Electrical Engineering Department, Amirkabir University of Technology, Tehran, Iran.
[2]Electrical Engineering Department, Faculty of Engineering, Bahonar University, Kerman, Iran.
[3]Electrical Engineering Department, Zanjan University, Zanjan, Iran.
[4]Department of Electrical and Computer Engineering, University of Florida, Gainesville, Florida.

Paper number 2000JD900541.
0148-0227/00/2000JD900541$09.00

Table 1. Mathematical Descriptions of Four "Engineering" Models and Values of Their Parameters Used in This Paper

Model	Mathematical Description for Current
TL	$i(z',t)=\begin{cases} i(0,t-z'/v) & z' \le vt \\ 0 & z' > vt \end{cases}$ $v = 1.3\times10^8$ m/s
MTLL	$i(z',t)=\begin{cases} (1-\frac{z'}{H})\, i(0,t-z'/v) & z' \le vt \\ 0 & z' > vt \end{cases}$ $v = 1.3\times10^8$ m/s, H = 7 km
MTLE	$i(z',t)=\begin{cases} e^{-z'/\lambda}\, i(0,t-z'/v) & z' \le vt \\ 0 & z' > vt \end{cases}$ $v = 1.3\times10^8$ m/s, λ = 2 km
DU	$i(z',t)=\begin{cases} i(0,t+z'/c)-i(0,z'/v+z'/c)e^{-(t-z'/v)/\tau_d} & z' \le vt \\ 0 & z' > vt \end{cases}$ $v = 1.3\times10^8$ m/s, $c = 3\times10^8$ m/s $\tau_d = 0.6^*$ μs

*Only one discharge time constant is used, which is sufficient for computing fields during the first 5-10 μs [*Diendorfer and Uman*, 1990]. Note that *Thottappillil and Uman* [1993] and *Thottappillil et al.* [1997] also used a single discharge time constant τ_d, but its value was 0.1 μs.

et al., 1997]. The DU model provides a reasonably good match between the model-predicted and measured electromagnetic fields and it introduces current dispersion (change of the shape of current waveform as it propagates along the channel), but the specification of the dispersion is arbitrary. The waveshape characteristics of the remote fields predicted by the DU model are very sensitive to variations in the shape of the channel-base current [e.g., *Thottappillil et al.*, 1991].

For a straight channel oriented along the *z* axis, the expressions for current distribution along the channel predicted by TL, MTLL, MTLE, and DU models are summarized in Table 1. Once the spatial-temporal distribution of the channel current is determined, the remote electric and magnetic fields can be easily calculated [e.g., *Rakov and Uman*, 1998].

In this paper a new model, based on antenna theory, i.e., on a complete solution of Maxwell's equations, is presented and used to obtain the channel current and charge density profiles. According to the classification of return-stroke models proposed by *Rakov and Uman* [1998], the antenna-theory (AT) model belongs to the class of electromagnetic models. In the AT model, the lightning return-stroke channel is represented by a vertical, lossy monopole antenna above a perfectly conducting ground. The antenna is fed at its lower end by a source whose voltage is determined using the assumed antenna input current waveform and the resistance of antenna per unit length, as described in the Appendix. The source launches a current wave along the antenna, which radiates electromagnetic fields into a nonconducting medium whose electrical permittivity is selected such that the wave propagates at a specified speed (lower than the speed of light). The artificial change of permittivity is used to account for the effect of corona on the wave propagation speed. The distribution of current along the antenna is determined applying the boundary condition for the tangential component of electric field on the surface of the antenna. The solution is found numerically, using the method of moments, with ohmic losses in the antenna being taken into account by introducing the resistive loading (series resistance per unit length). Nonlinear effects associated with the dependences of the shunt capacitance of the lightning channel on its electric potential and of the series resistance on longitudinal lightning current are neglected. The resultant distribution of current along the antenna is allowed to radiate into free space.

In the AT model, only two adjustable parameters are needed, the propagation speed of the current wave for a nonresistive channel and the resistance per unit channel length. The evolution of the current and charge along the channel is described by Maxwell's equations.

2. General Theoretical Approach

The starting point of the analysis is the time domain Maxwell's equations for a linear, homogenous, and time invariant medium,

$$\begin{aligned} \nabla\times\mathbf{E} &= -\mu\frac{\partial\mathbf{H}}{\partial t}, \\ \nabla\times\mathbf{H} &= \mathbf{J}+\varepsilon\frac{\partial\mathbf{E}}{\partial t}, \\ \nabla\cdot\mathbf{E} &= \frac{\rho}{\varepsilon}, \\ \nabla\cdot\mathbf{H} &= 0, \end{aligned} \tag{1}$$

where ε and μ are the electric permittivity and magnetic permeability of medium, **E** and **H** are the electric and magnetic field intensities, and **J** and ρ are the volume current and charge densities, respectively. The relation between **J** and ρ is specified by the current continuity equation

$$\nabla\cdot\mathbf{J} = -\frac{\partial\rho}{\partial t}. \tag{2}$$

Combining Maxwell's equations yields the following expressions (wave equations):

$$\begin{aligned} \nabla^2\mathbf{E}(\mathbf{r},t)-\frac{1}{c^2}\frac{\partial^2}{\partial t^2}\mathbf{E}(\mathbf{r},t) &= \mu\frac{\partial\mathbf{J}}{\partial t}(\mathbf{r},t)+\frac{1}{\varepsilon}\nabla\rho(\mathbf{r},t), \\ \nabla^2\mathbf{H}(\mathbf{r},t)-\frac{1}{c^2}\frac{\partial^2}{\partial t^2}\mathbf{H}(\mathbf{r},t) &= -\nabla\times\mathbf{J}(\mathbf{r},t), \end{aligned} \tag{3}$$

where **r** is the position vector of a point in space. If we consider a perfectly conducting antenna (later we will introduce resistive loading) in a homogenous medium, the volume current and charge densities, **J** and ρ, can be replaced by the surface current and charge densities, $\mathbf{J}_s$ and ρ_s,

$$\begin{aligned} \mathbf{J}(\mathbf{r},t) &= \mathbf{J}_s(\mathbf{r}_0,t)\delta_s(\mathbf{r}-\mathbf{r}_0), \\ \rho(\mathbf{r},t) &= \rho_s(\mathbf{r}_0,t)\delta_s(\mathbf{r}-\mathbf{r}_0), \end{aligned} \tag{4}$$

in which $\mathbf{r}_0$ is the position vector of a point on the surface of the antenna, and δ_s is the two-dimensional impulse function

$$\delta_s(\mathbf{r}-\mathbf{r}_0)=\begin{cases}\infty & \text{if } \mathbf{r}=\mathbf{r}_0 \\ 0 & \text{otherwise.}\end{cases}$$

The Green's solution (G) of a nonhomogeneous wave equation

$$\nabla^2 G-\frac{1}{c^2}\frac{\partial^2 G}{\partial t^2} = -\delta(\mathbf{r}-\mathbf{r}_0)\delta(t-t_0), \tag{5}$$

where

$$\delta(\mathbf{r}-\mathbf{r}_0)=\delta(x-x_0)\delta(y-y_0)\delta(z-z_0)$$

is given by *Stratton* [1941]:

$$G(\mathbf{r},\mathbf{r}_0,t-t_0)=\frac{1}{4\pi}\frac{\delta(t-t_0-R/c)}{R}. \tag{6}$$

In this equation, $R = |\mathbf{r} - \mathbf{r}_0|$; $\mathbf{r}_0$ is the spatial location, and t_0 is the initial temporal point of the source (current or charge density on the surface of the conductor).

Applying the above solution to equations (3), we obtain the radiated fields produced by surface current density $\mathbf{J}_s$ [*Reinex*, 1986],

$$\mathbf{E}(\mathbf{r},t)=-\iint_{S_0}\left[\mu\frac{\partial \mathbf{J}_s}{\partial t}(\mathbf{r}_0,t)\underset{(t)}{*}G(\mathbf{r},\mathbf{r}_0,t)+\frac{1}{\varepsilon}\int_0^t\nabla\cdot\mathbf{J}_s(\mathbf{r}_0,\tau)d\tau \underset{(t)}{*}\nabla_0 G(\mathbf{r},\mathbf{r}_0,t)\right]ds_0, \tag{7}$$

$$\mathbf{H}(\mathbf{r},t)=\iint_{S_0}\mathbf{J}_s(\mathbf{r}_0,t)\underset{(t)}{\hat{*}}\nabla_0 G(\mathbf{r},\mathbf{r}_0,t)\,ds_0 .$$

The subscript (t) refers to convolution operator variable (time), and the subscript zero is related to the differentiation variable ($\mathbf{r}_0$). The symbol $\underset{(t)}{\hat{*}}$ denotes the cross product with respect to space and convolution in time, and integration is performed over the outer surface of the antenna (S_0).

The response of a monopole antenna (see Figure 1) above a perfectly conducting ground to an electromagnetic wave produced by an external source can be found considering the scattering of electromagnetic fields by a metallic object. The boundary condition on the surface of a perfect conductor can be expressed as

$$\mathbf{n}\times(\mathbf{E}^a+\mathbf{E})=0, \tag{8}$$

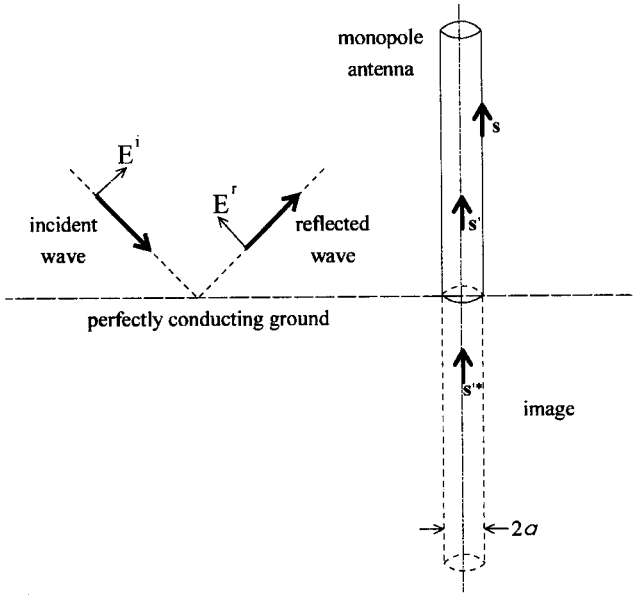

Figure 1. Geometry of vertical monopole antenna in receiving mode located above a perfectly conducting ground. In transmitting mode, the excitation field is nonzero only at the base of the antenna. See text for details.

where $\mathbf{E}^a$ is the applied field, and $\mathbf{n}$ is the normal vector to the surface of conducting object. For a nonideal conductor, the right-hand side of equation (8) is not equal to zero and depends on resistance per unit length. Combining (7) and (8), we have

$$\mathbf{n}\times\mathbf{E}^a(\mathbf{r},t)=\mathbf{n}\times \mathrm{Vp}\iint_{S_0}\left[\mu\frac{\partial \mathbf{J}_s}{\partial t}(\mathbf{r}_0,t)\underset{(t)}{*}G(\mathbf{r},\mathbf{r}_0,t)+\frac{1}{\varepsilon}\int_0^t\nabla\cdot\mathbf{J}_s(\mathbf{r}_0,\tau)d\tau\underset{(t)}{*}\nabla_0 G(\mathbf{r},\mathbf{r}_0,t)\right]ds_0. \tag{9}$$

In equation (9), Vp is the principal value of the integral operator [*Bouix*, 1964]. In the case of homogenous, linear, and time-invariant media, inserting equation (6) into (9) will yield the following equation:

$$\mathbf{n}\times\mathbf{E}^a(\mathbf{r},t)=\frac{\mathbf{n}}{4\pi}\times \mathrm{Vp}\iint_{S_0}\left[\frac{\mu}{R}\frac{\partial \mathbf{J}_s}{\partial t}(\mathbf{r}_0,t)+\frac{\mathbf{R}}{\varepsilon cR^2}\nabla\cdot\mathbf{J}_s(\mathbf{r}_0,t-R/c)+\frac{\mathbf{R}}{\varepsilon R^3}\int_0^t\nabla\cdot\mathbf{J}_s(\mathbf{r}_0,\tau)d\tau\right]ds_0, \tag{10}$$

where $\mathbf{R} = \mathbf{r} - \mathbf{r}_0$.

We will use the thin-wire approximation [*Miller et al.*, 1973] according to which the current $I(s,t)$ on a wire structure of radius a satisfies the equations,

$$I(s,t)=2\pi a J(s,t),\qquad \mathbf{J}(s,t)=\frac{I(s,t)}{2\pi a}\mathbf{s}, \tag{11}$$

where s is the location of a point on the wire structure and $\mathbf{s}$ is the corresponding tangential unit vector (see Figure 1).

Because of the presence of ground the total excitation (or applied) field produced by the source above ground is

$$\mathbf{E}^a=\mathbf{E}^i+\mathbf{E}^r, \tag{12}$$

where $\mathbf{E}^i$ is the incident field and $\mathbf{E}^r$ is the reflected field from the ground. The excitation field $\mathbf{E}^a$ induces current I ($\mathbf{s}$, t) at each point of the antenna. According to equation (10) and thin-wire approximation (11), this current will produce the scattered field $\mathbf{E}$, which can be described in the following form:

$$\mathbf{E}(\mathbf{s},t)=\mathbf{L}[I(\mathbf{s},t)], \tag{13}$$

where $\mathbf{L}$ is an integrodifferential operator [*Herault et al.*, 1990]. Note that $\mathbf{E}^a$ is independent of the presence of the antenna, and $\mathbf{E}$ can be viewed as a reaction of the antenna to $\mathbf{E}^a$. For the receiving antenna mode, illustrated in Figure 1, $\mathbf{E}^a$ is produced by an external source and exists everywhere in space. For the transmitting antenna mode, $\mathbf{E}^a$ is produced by a lumped source connected between the lower end of the antenna and the ground and is zero everywhere except for the position of the source. Similar to the receiving mode, $\mathbf{E}^a$ is totally independent of the presence of antenna. The source, whose voltage is related to $\mathbf{E}^a$ as described later in this section, launches a current wave along the antenna. Electric field produced by this current wave is scattered field $\mathbf{E}$ which, similar to the receiving mode, can be viewed as a reaction of the antenna to $\mathbf{E}^a$.

The continuity of tangential component of the total electric field at any point on the antenna surface requires that

$$\mathbf{s}\cdot\left(\mathbf{E}^a(\mathbf{s},t)+\mathbf{L}[I(\mathbf{s},t)]\right)=0, \tag{14}$$

which is the same as equation (8). As stated above for equation (8), for a nonideal conductor the right-hand side of equation (14) is not equal to zero. Using the definition of the **L** operator and the thin-wire approximation [*Herault et al.*, 1990; *Moini et al.*, 1998], we can write

$$\mathbf{s}\cdot\mathbf{E}^a(\mathbf{s},t)=\frac{\mu_0}{4\pi}\int_{C_0}\left[\frac{\mathbf{s}\cdot\mathbf{s}'}{R}\frac{\partial}{\partial t'}I(\mathbf{s}',t')+v\frac{\mathbf{s}\cdot\mathbf{R}}{R^2}\frac{\partial}{\partial s'}I(\mathbf{s}',t')\right.$$
$$+v^2\frac{\mathbf{s}\cdot\mathbf{R}}{R^3}\int_0^{t'}\left(\frac{\partial}{\partial s'}I(\mathbf{s}',\tau)\,d\tau\right)$$
$$-\frac{\mathbf{s}\cdot\mathbf{s}'^*}{R^*}\frac{\partial}{\partial t'^*}I(\mathbf{s}',\mathbf{t}'^*)-v\frac{\mathbf{s}\cdot\mathbf{R}^*}{R^{*2}}\frac{\partial}{\partial s'}I(\mathbf{s}',t'^*)$$
$$\left.-v^2\frac{\mathbf{s}\cdot\mathbf{R}^*}{R^{*3}}\int_0^{t'^*}\frac{\partial}{\partial s'}I(\mathbf{s}',\tau)\,d\tau\right]ds', \tag{15}$$

where

$$R=(|\mathbf{s}-\mathbf{s}'|^2+a^2)^{1/2},$$
$$R^*=(|\mathbf{s}-\mathbf{s}'^*|^2+a^2)^{1/2},$$
$$c=\frac{1}{\sqrt{\varepsilon_0\mu_0}},$$
$$t'=t-\frac{R}{v},\ t'^*=t-\frac{R^*}{v}.$$

C_0 is the path along which the current is flowing, a is the radius of the antenna (Figure 1), and v is the wave propagation speed for the case of nonresistive channel. As explained later, we assume that $v=c/\sqrt{\varepsilon_r}$, where $\varepsilon_r=\varepsilon/\varepsilon_0$ is the assumed relative electric permittivity; the actual value of the propagation speed is slightly reduced with respect to v due to ohmic losses in the antenna. Further, s and s' are the observation and source points on the antenna, respectively, s'* is the image of the source point s', and **s**, **s'**, and **s'*** are the corresponding unit tangential vectors. The last three terms in the right-hand side of equation (15) represent the effect of perfect ground. The left-hand side of equation (15) represents the applied (excitation) electric field, tangential to the surface of the antenna. For the case of transmitting antenna, the applied field $\mathbf{E}^a(\mathbf{s},t)$ is produced by a voltage source (not shown in Figure 1 which illustrates the receiving antenna mode). The relation between $\mathbf{E}^a(\mathbf{s},t)$ and source voltage $v(\mathbf{s},t)$ according to *Herault et al.* [1990] is

$$\mathbf{E}^a(\mathbf{s},t)=\begin{cases}-\nabla v(\mathbf{s}',t) & \text{if } \mathbf{s}=\mathbf{s}'=0\\ 0 & \text{elsewhere.}\end{cases} \tag{16}$$

The numerical solution of equation (15), the electric field integral equation (EFIE), by the method of moments (MOM) in the time domain [*Miller et al.*, 1973] yields the time-space distribution of current along the antenna. In using the method of moments, a set of rectangular basis functions is defined for expressing the unknown current in each of the segments of the antenna, and a second-order polynomial representation is used to evaluate the current. The last step of the method of moments is choosing the test functions in order to get a system of linear equations. The point-matching method based on Dirac distributions [*Herault et al.*, 1990] is utilized.

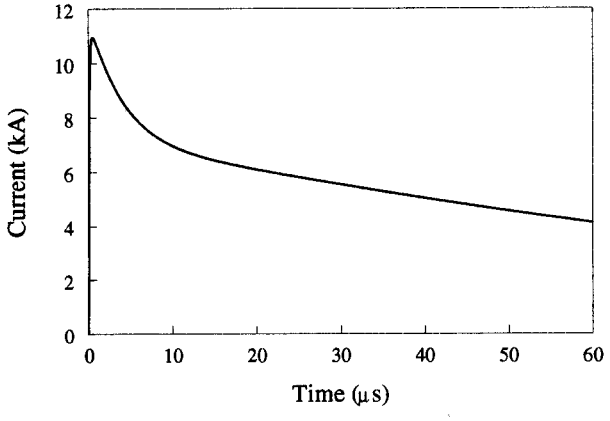

Figure 2. Channel-base current waveform used for the comparison of different models in this paper. The peak current is about 11 kA, and peak current rate of rise is about 105 kA/μs. Adapted from *Nucci et al.* [1990].

3. Antenna Theory (AT) Model

In this model, the return-stroke channel is considered as a lossy vertical antenna fed by a voltage source at its lower end, while for "engineering" models, the input to the model is a current waveform at the base of the channel. In order to compare "engineering" models with the AT model quantitatively, we need to use the same input current in all the models. This means that the voltage source for the monopole antenna should produce the same current as the channel-base current assumed in the "engineering" models. The voltage of the source is given by the following equation:

$$v(t)=\mathrm{F}^{-1}\left[Z(f)\cdot I(0,f)\right], \tag{17}$$

where $I(0,f)$ is the Fourier transform of the specified channel-base current, $Z(f)$ is the input impedance of the lossy monopole antenna, and F^{-1} denotes the inverse Fourier transform. The input impedance of the monopole antenna, which is a function of its length and distributed resistance, is calculated applying the method of moments (MOM) to the electric field integral equation (EFIE). The details of evaluation of the voltage source waveform are described in the Appendix. Once the voltage $v(t)$ of the source is determined, the corresponding applied electric field $\mathbf{E}^a$, to be substituted in equation (15), is estimated as the ratio of this voltage and the length Δz of the excitation (source) segment of the antenna.

To reduce the propagation speed of the current wave in the AT model to a value consistent with observations, $v < 3\times10^8$ m/s, we use $\varepsilon > \varepsilon_0$ in calculating the current variation along the channel, and then use that current distribution to calculate the electromagnetic fields radiated by the antenna in free space ($\varepsilon = \varepsilon_0$). The arbitrary increasing of ε in determining the channel current distribution serves to account for the fact that channel charge is predominantly stored in the radial corona sheath whose radius is much larger than that of the channel core which carries the longitudinal channel current, resulting in $v < 3\times10^8$ m/s. This simulates an increase of shunt capacitance per unit antenna length due to corona. The use of $\varepsilon > \varepsilon_0$ additionally introduces the effect of radiation into the fictitious medium, but the resultant current distribution along the channel is unlikely to differ significantly from the case of no such effect (the transmission line current is expected to dwarf the antenna current). An alternative approach to modeling corona effect on propagation speed would be to introduce capacitive antenna loading. ohmic losses in the antenna

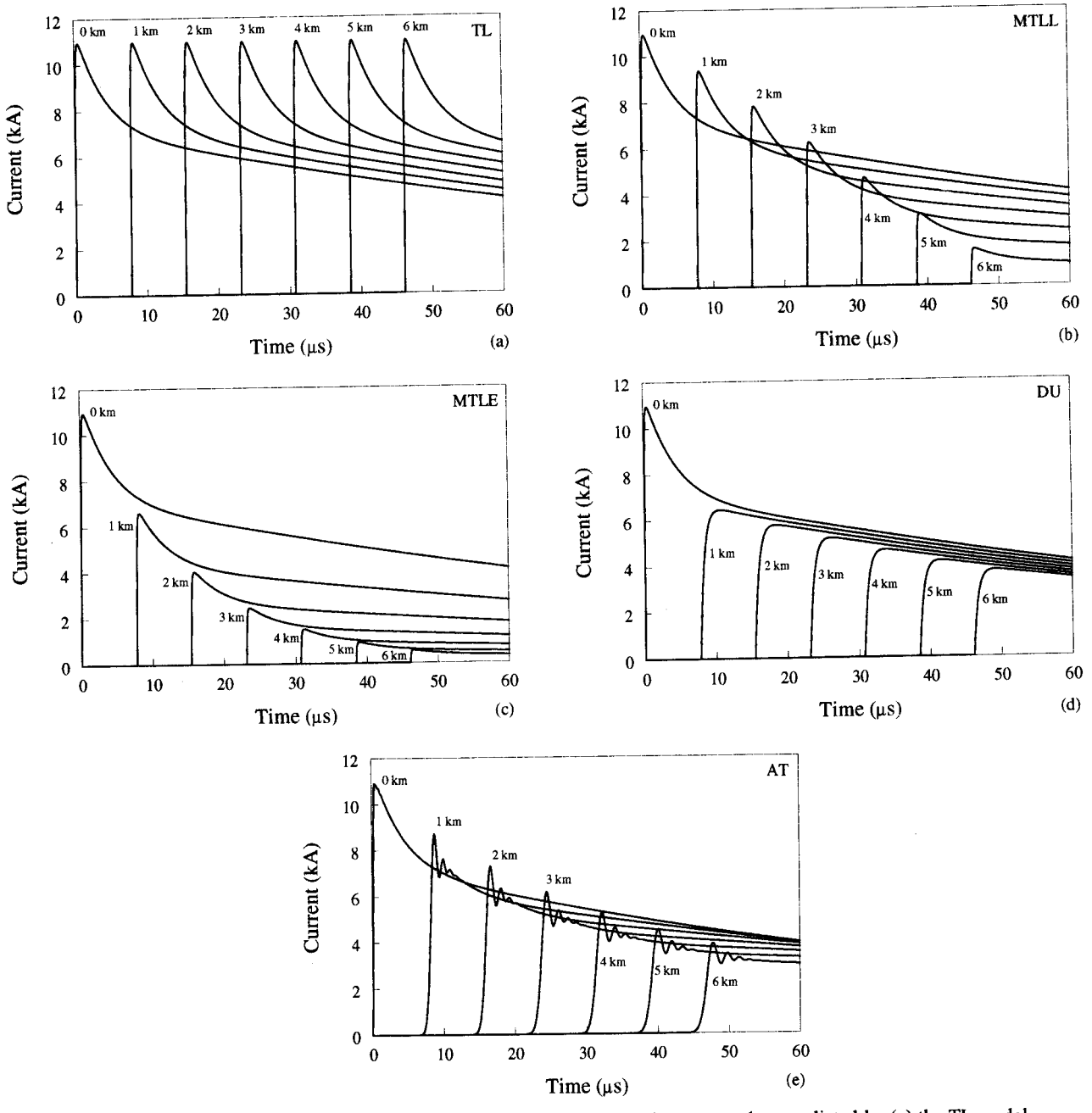

Figure 3. Channel current as a function of time at different heights above ground as predicted by (a) the TL model, (b) the MTLL model, (c) the MTLE model, (d) the DU model, and (e) the AT model. For the AT model it is assumed that $\varepsilon_r = 5.3$ and $R = 0.07\ \Omega/m$.

further reduce v, but for the selected value of resistance per unit length (see below), this additional reduction in v is expected to be relatively small. In the AT model, there are only two parameters to be adjusted, the propagation speed v for the case of nonresistive antenna and the value of distributed resistance R (not to be confused with distance R in equation (6)). The value of resistance per unit length was selected (by trial and error) to provide an agreement between model-predicted and measured electric fields at close distances. It was assumed for the AT model that $R = 0.07\ \Omega/m$ (see Appendix) and that $v = 1.3 \times 10^8$ m/s, which corresponds to $\varepsilon_r = 5.3$. As stated above, the spatial and temporal distribution of current along the antenna was determined solving the EFIE, equation (15), using MOM. The computation time on a Pentium computer with 128 MB RAM is about 5 min.

4. Comparison of Models

In the following, we compare the AT model with other models in terms of (1) spatial and temporal current distribution, (2) line charge density distribution, and (3) remote electromagnetic fields. In doing so, we assume the same lightning channel-base current waveform as that used by *Nucci et. al.* [1990], *Rakov and Dulzon* [1991], and *Thottappillil et. al.* [1997]. This waveform is depicted in Figure 2.

4.1. Current Distribution

Current waveforms as a function of time at different heights along the channel for five models, the TL, MTLL, MTLE, DU, and AT models, are compared in Figure 3. For the TL model the

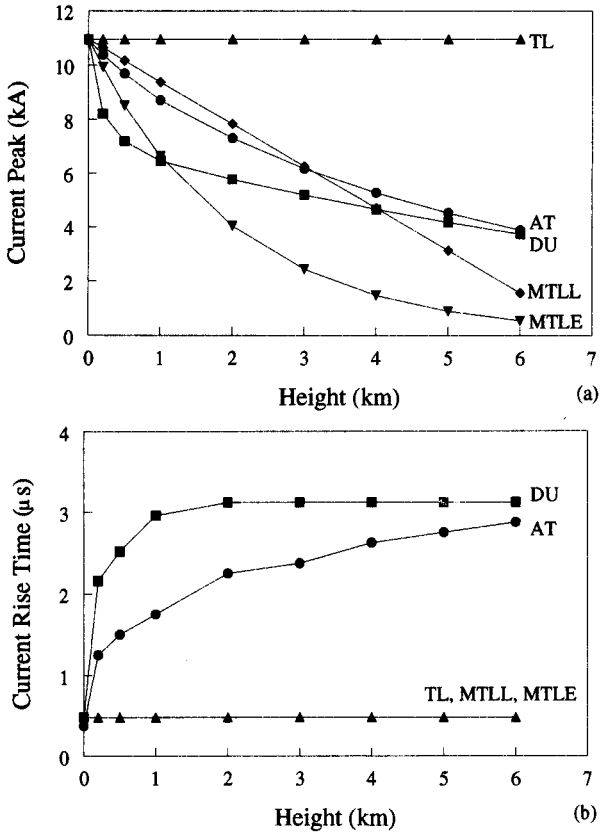

Figure 4. (a) Current peak as a function of height predicted by the TL, MTLL, MTLE, DU, and AT models. (b) Current risetime to peak as a function of height predicted by the TL, MTLL, MTLE, DU, and AT models.

current waveforms at different heights are the same, and for the MTLL and MTLE models, the current amplitude decreases with height, while the waveshape remains the same. For the DU model both attenuation and dispersion of current waveform are observed. The current peak and current risetime each as a function of height for the five models are shown in Figure 4. For the TL model, neither current peak nor current risetime changes with height. The MTLL and MTLE models are characterized by linear and exponential decrease of the current peak with height, respectively, while the current risetime remains the same at all heights. For the AT model, the variation of current peak with height within the lowest 4 km or so of the channel is similar to that for the MTLL model. Both the DU and the AT models are characterized by the increase of current risetime with height, but for the DU model, the pronounced increase occurs only within the lowest 1 km or so of the channel. Note that for the AT model the current peak decreases with height due to both ohmic losses in the antenna and radiation losses; that is, a decrease of current peak with increasing height would be observed even if the ohmic losses were neglected.

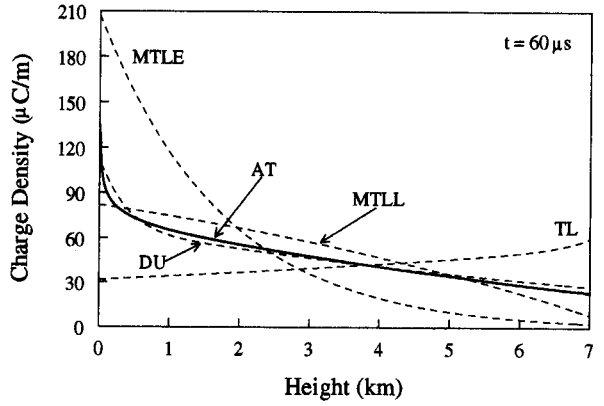

Figure 5. Line charge density distribution along the channel calculated for different models at t = 60 μs.

4.2. Line Charge Density Distribution

The line charge density at any height z' on a straight vertical lightning channel at any time t is given by [*Thottappillil et al.*, 1997]

$$\rho_L(z',t) = \frac{i(z',z'/v)}{v} - \int_{z'/v}^{t} \frac{\partial i(z',\tau)}{\partial z'} d\tau . \qquad (18)$$

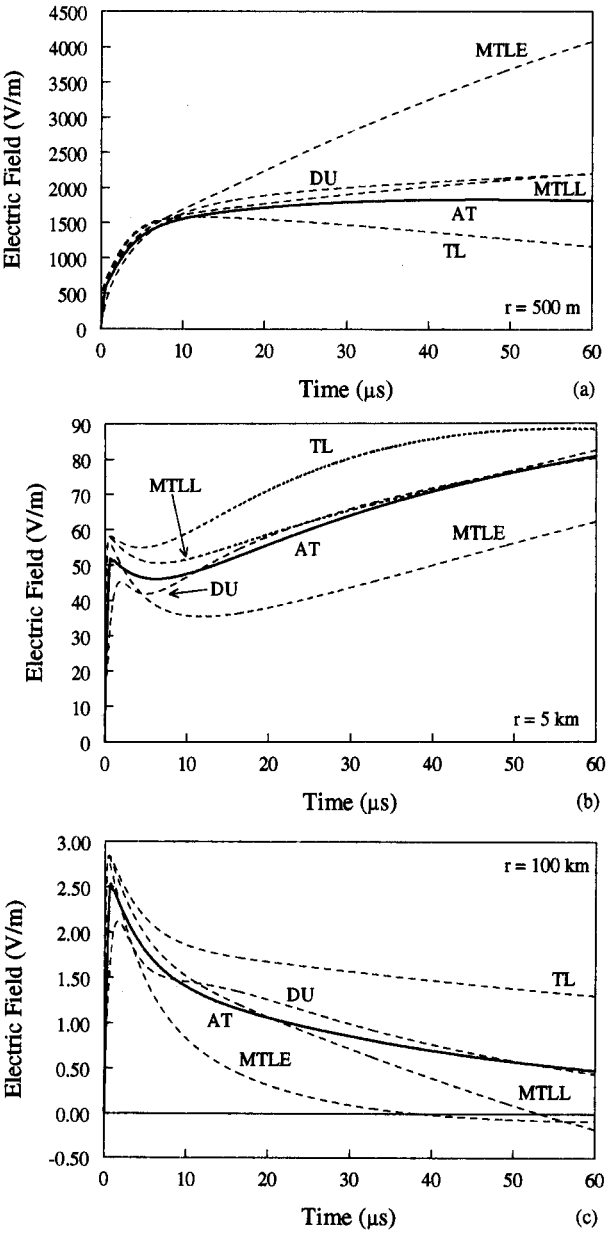

Figure 6. Vertical component of electric field calculated at different distances (r) from the channel: (a) r = 500 m, (b) r = 5 km, (c) r = 100 km.

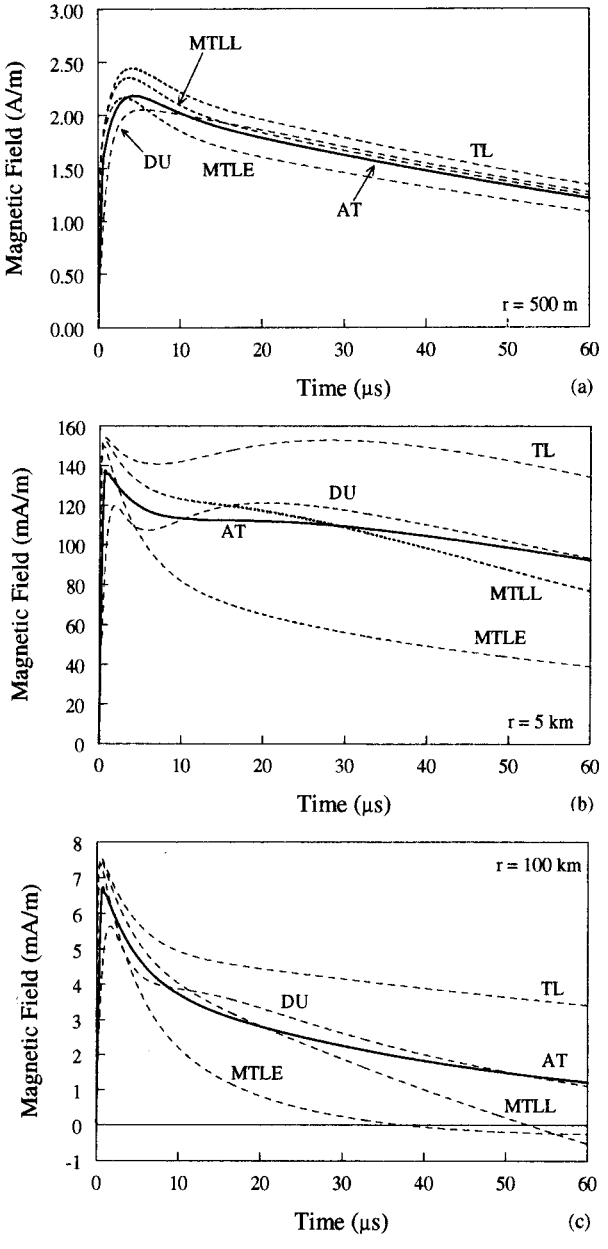

Figure 7. Horizontal component of magnetic field calculated at different distances (r) from the channel: (a) r = 500 m, (b) r = 5 km, (c) r = 100 km.

The first term of (18) represents only the deposited charge density component, while the second term can contribute to both transferred and deposited charge density components, the two components being defined by *Thottappillil et al.* [1997]. Applying the Leibnitz formula to (18), we obtain

$$\rho_L(z',t) = -\frac{d}{dz'}\int_{z'/v}^{t} i(z',\tau)d\tau \,. \qquad (19)$$

Equation (19) has been applied to five return-stroke models, and the resultant charge density profiles at t = 60 μs are shown in Figure 5. For the TL model there is no deposited charge, and the total charge density is equal to transferred charge density which becomes equal to zero when the current ceases to flow in all channel sections of interest [*Thottappillil et al.*, 1997]. For the other four models, the total charge density at 60 μs is a combination of transferred and deposited charge density components. When the current ceases to flow everywhere in the channel, the transferred charge density component becomes zero and the total charge density becomes equal to the deposited charge density component. As seen in Figure 5, the MTLE model has a total charge density near ground 2 to 3 times higher than that predicted by the AT, MTLL, and DU models. This disparity translates into an appreciable difference in the model-predicted return stroke electric fields at close ranges, as shown in section 4.3.

4.3. Remote Electromagnetic Fields

Figures 6 through 9 illustrate the calculated electric and magnetic fields at various distances from the channel, displayed on two different timescales. The fields were computed using traditional equations found, for example, in the work of *Rakov and Uman* [1998]. Due to computer memory limitation, the calculations were performed only up to 60 μs, and for the AT

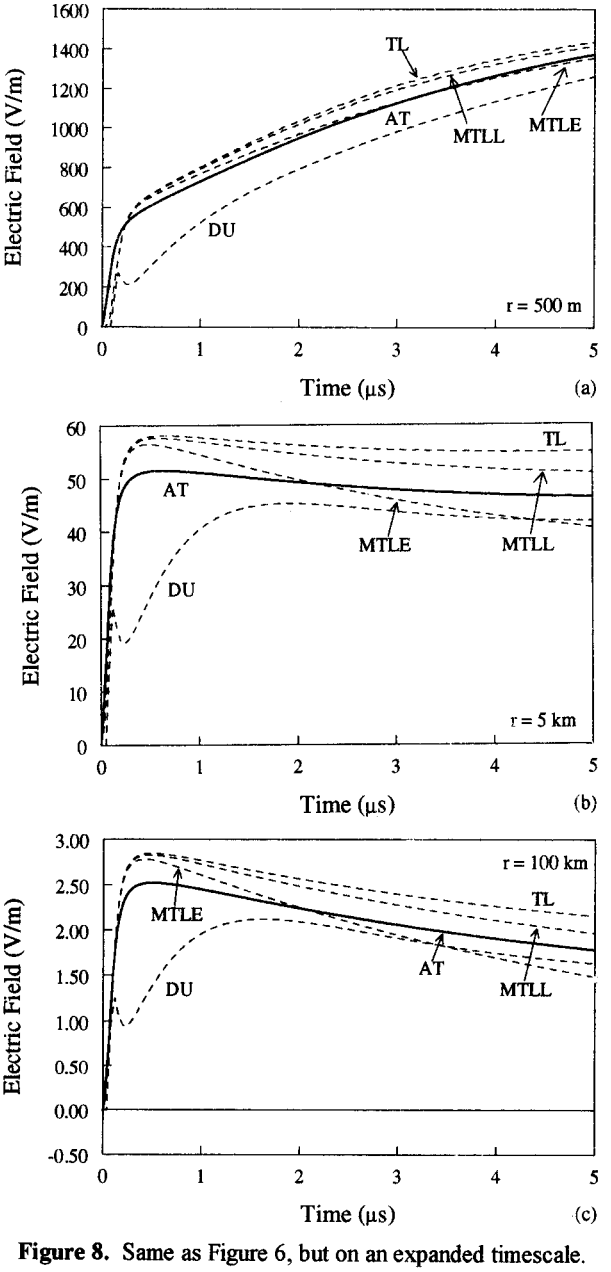

Figure 8. Same as Figure 6, but on an expanded timescale.

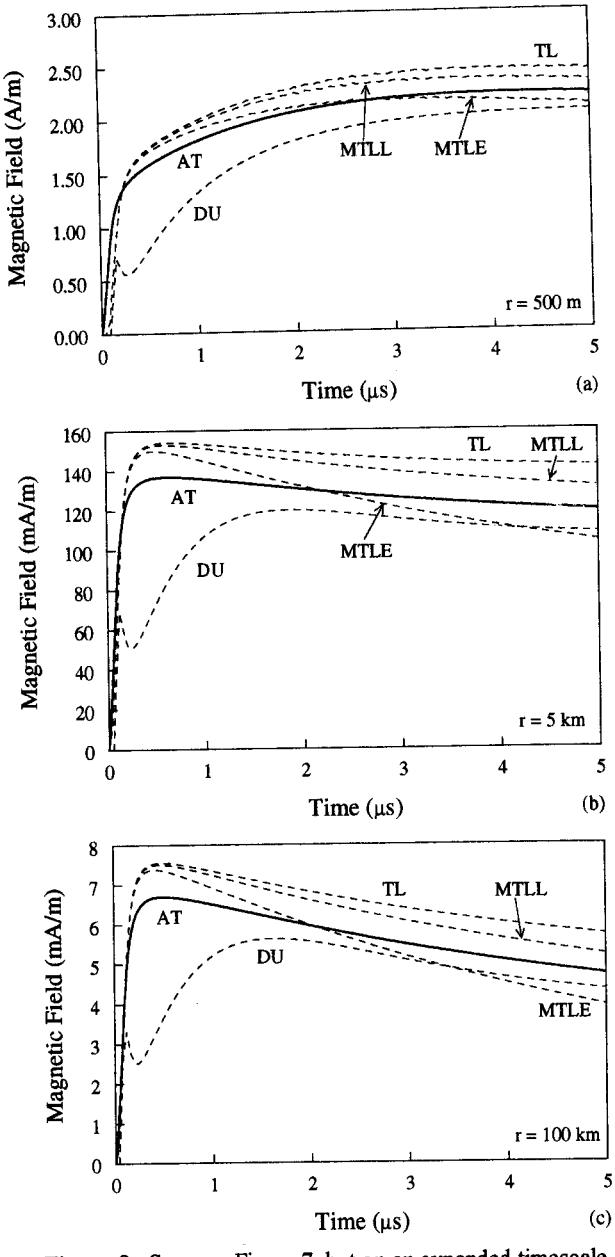

Figure 9. Same as Figure 7, but on an expanded timescale.

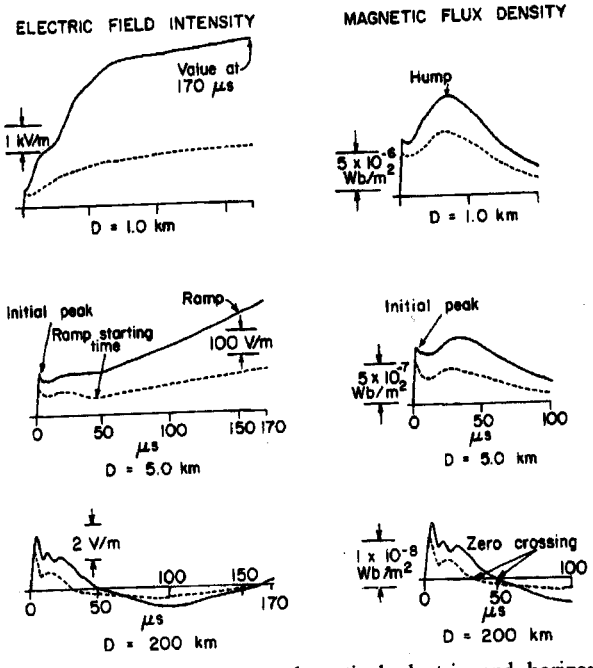

Figure 10. Typical measured vertical electric and horizontal magnetic fields at various distances from the channel. Adapted from *Lin et al.* [1979].

model the channel segment length Δz was 15 m. The calculated fields can be compared with typical measured ones shown in Figure 10. Except for the TL and MTLE models, the 500 m electric field waveforms predicted by all the models are more or less consistent with experimental data. In particular, the electric fields predicted by the MTLL, DU, and AT models show little variation after 10 μs or so, following the initial relatively rapid change, in keeping with observations. At 5 km the electric field exhibits a ramp after the initial peak for all the models, except for the TL model [see also *Nucci et. al.* 1990]. In fact, at distances of the order of some kilometers, the TL model allows the reproduction of only the first few tens of microseconds of the characteristic electric field ramp observed in the experimental data to last for more than a hundred of microseconds. Note that at distances greater than a few kilometers the initial rapid transition in electric field is reasonably reproduced by all the models, because (1) this feature is formed when the current wave is very close to the ground and (2) the same current waveform at ground level is assumed for all models. In contrast with the other models, the DU model predicts a nonmonotonic rise to the initial peak (a spike within the first some hundreds of nanoseconds), as seen in

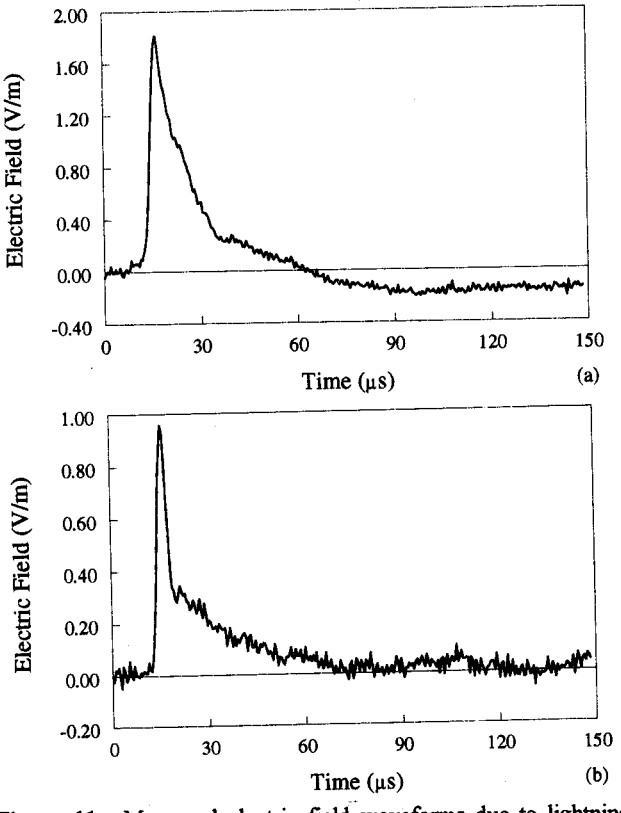

Figure 11. Measured electric field waveforms due to lightning discharges at distances of about 250 km in Florida. Note that one of the waveforms (a) shows a zero crossing, while the other one (b) does not. See text for details.

Figures 8 and 9. At far distances from the channel base, e.g., r = 100 km, all the models predict more or less similar field peak values. On the other hand, the MTLL and MTLE models predict a zero crossing after a few tens of microseconds, a feature generally considered to be characteristic of distant fields [*Lin et al.*, 1979], while the TL, DU, and AT models do not do so. In summary, it appears that the TL model is not a realistic model for calculating lightning electric fields at times greater than some tens of microseconds at distances of the order of some kilometers (see also *Nucci et al.* [1990]) and after only a few microseconds at distances of the order of tens of meters from the channel (see *Thottappillil et al.* [1997]). The MTLL-model-predicted fields are consistent with observed fields at all ranges. The MTLE model is incapable of reproducing adequately the observed electric field waveforms at very close (tens to hundreds of meters) ranges (see also *Thottappillil et al.* [1997]). The DU and AT models do not reproduce the zero crossing at far ranges. However, this latter feature depends on the assumed channel-base current waveform (see also *Thottappillil et al.* [1991]), in particular, on the rate of decrease of current after the peak and on channel geometry. Indeed, the field zero crossing occurs when the contribution from the leading positive and trailing negative portions of the spatial current derivative wave become equal in magnitude, the time of this event being a function of channel inclination with respect to the observer. As an example, we present in Figure 11 electric field waveforms measured at distances of about 250 km in Florida, one of which showing and the other not showing zero crossing within 100 μs of the initial peak. Note that the two waveforms were apparently produced in the same thunderstorm within less than 3 min of each other.

5. Summary

A new antenna theory (AT) model for the lightning return stroke is introduced. In this model, the lightning channel is represented by a lossy vertical monopole antenna, which is fed at its lower end by a voltage source. The voltage waveform is specified on the basis of the assumed input current of the antenna and antenna resistance per unit length. There are only two adjustable parameters in this model: the wave propagation speed for a nonresistive channel and the value of the distributed channel resistance. Once these two parameters are specified, the spatial and temporal distribution of the current along the channel is found by solving the electric field integral equation (derived from Maxwell's equations in the time domain), using the method of moments. The AT model was compared with other return-stroke models in terms of current and line charge density distributions along the channel, and the predicted remote electromagnetic fields. The primary features of the antenna theory model are as follows: (1) the current amplitude decreases and current risetime increases as the current wave propagates along the channel, in agreement with optical observations, (2) the current wave propagates along the channel at a speed lower than the speed of light due to both the effect of corona and ohmic losses in the channel, and (3) the model-predicted electric and magnetic fields are reasonably consistent with typical measured fields. The AT model can easily be extended to include arbitrary channel geometry, strike object, and the electromagnetic coupling between the return-stroke channel and any wire structure located in the vicinity of the channel (e.g., power or communication line).

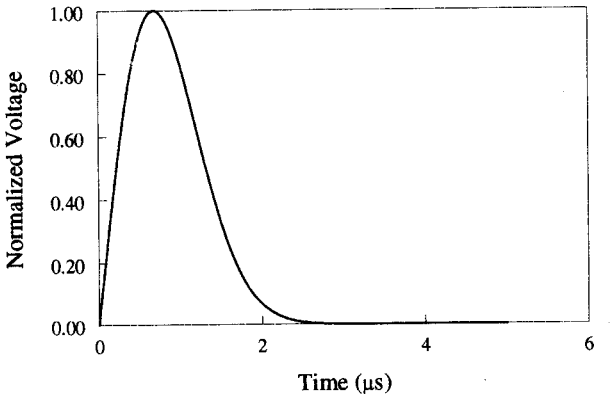

Figure A1. Normalized modulated Gaussian waveform in the time domain which has been used as a source voltage to calculate the input impedance of the monopole antenna.

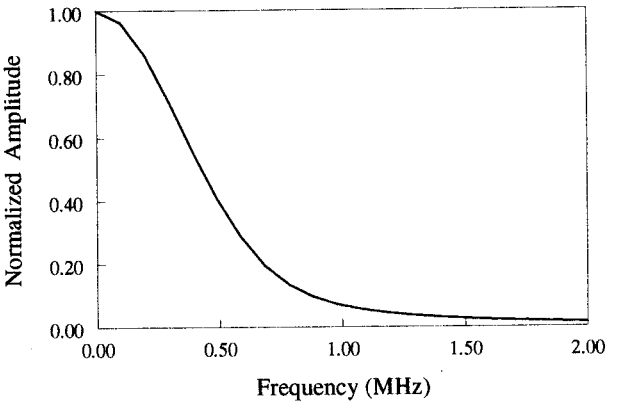

Figure A2. Normalized amplitude of the modulated Gaussian waveform in the frequency domain corresponding to the time domain waveform shown in Figure A1.

Appendix

The voltage $v(t)$, exciting the monopole antenna, which results in the specified channel-base current, is evaluated using the following equation:

$$v(t) = \mathrm{F}^{-1}\left[Z(f)\cdot I(0,f)\right]. \qquad \text{(A1)}$$

In this equation, $Z(f)$ is the input impedance of the monopole antenna in the frequency domain, and $I(0,f)$ is the Fourier transform of the channel-base current. To find the input impedance of the monopole antenna, a modulated Gaussian waveform, shown in Figure A1, was used. Figure A2 depicts this waveform in frequency domain. Using equation (16) and solving the electric field integral equation (equation (15)) by the method of moments, which allowed to include resistive loading, we obtained the input current of the monopole antenna corresponding to the modulated Gaussian voltage waveform. The input impedance of the antenna is then found by dividing the input voltage by the input current in the frequency domain. Figure A3 shows the source voltage, found using the computed input impedance and specified current at the channel base, for different values of resistance R per unit length. The waveform of the source voltage is almost independent of R during the first tenths of microseconds. The value of R = 0.07 Ω/m has been selected for the calculations presented in this paper, since this value provides the best agreement between model-predicted and observed

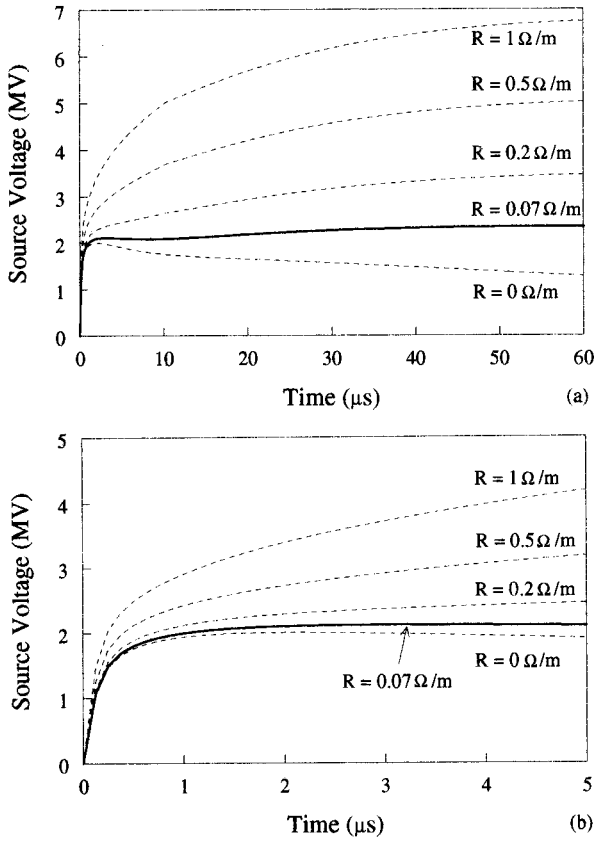

Figure A3. Calculated source voltage waveforms corresponding the channel-base current shown in Figure 2 for different values of the resistance per unit channel length. These waveforms are similar in their shapes to corresponding model-predicted electric field waveforms at some tens of meters from the lightning channel: (a) 60 μs timescale, (b) 5 μs timescale.

electric field waveforms at close (tens of meters) ranges. Interestingly, *Rakov* [1998] estimated the resistance per unit channel length to be 0.035 Ω/m behind the return-stroke front.

Acknowledgments. This study was supported in part by Amirkabir University Research grant 15/4139 and by NSF grants ATM 9415507 and 9726100. M. A. Uman, C. E. Baum, F. M. Tesche, and three anonymous reviewers provided a number of useful comments.

References

Bouix, M., *Les Fonctions Generalisees ou Distributions*, Masson, Paris, France, 1964.

Diendorfer, G., and M. A. Uman, An improved return-stroke model with specified channel-base current, *J. Geophys. Res.*, *95*, 13,621-13,644, 1990.

Herault, J., R. Moini, A. Reineix, and B. Jecko, A new approach to microstrip antenna using a mixed analysis: Transient-frequency, *IEEE Trans. Antennas Propagat.*, *38*, 1166-1175, 1990.

Lin, Y. T., M. A. Uman, J, A. Tiller, R. D. Brantley, W. H. Beasley, E. P. Krider, and C. D. Weidman, Characterization of lightning return stroke electric and magnetic fields from simultaneous two-station measurements, *J. Geophys. Res.*, *84*, 6307-6314, 1979.

Miller, E. K., A. J. Poggio, and G. J. Burke, An integrodifferential equation for time-domain analysis of thin wire structure, part I, *J. Comput. Phys.*, *12*, 24-48, 1973.

Moini, R., B. Kordi, and M. Abedi, Evaluation of LEMP effects on complex wire structures located above a perfectly conducting ground using electric field integral equation in time domain, *IEEE Trans. Electromagn. Compat.*, *40(2)*, 154-162, 1998.

Nucci, C.A., G. Diendorfer, M. A. Uman, F. Rachidi, M. Ianoz, and C. Mazzetti, Lightning return stroke current models with specified channel base current: A review and comparison, *J. Geophys. Res.*, *95*, 20,395-20,408, 1990.

Rakov, V. A., Some inferences on the propagation mechanisms of dart leaders and return strokes, *J. Geophys. Res.*, *103*, 1879-1887, 1998.

Rakov, V. A., and A. A. Dulzon, Calculated electromagnetic fields of lightning return strokes (in Russian), *Tekh. Elektrodin.*, *1*, 87-89, 1987.

Rakov, V. A., and A. A. Dulzon, A modified transmission line model for lightning return stroke field calculations, Proc. *Int. Zurich Symp. on Electromagn. Compat.*, *9*, 229-235, 1991.

Rakov, V. A., and M. A. Uman, Review and evaluation of lightning return stroke models including some aspects of their application, *IEEE Trans. Electromagn. Compat.*, *40(4)*, 403-426, 1998.

Reineix, A., Analyse theorique de la diffaraction d'ondes electromagnetiques impulsionnells, Doctorat, Univ. de Limoges, France, 1986.

Stratton, J. D., *Electromagnetic Theory*, McGraw-Hill, New York, 1941.

Thottappillil, R., and M. A. Uman, Comparison of lightning return-stroke models, *J. Geophys. Res.*, *98*, 22,903-22,914, 1993.

Thottappillil, R., M. A. Uman, and G. Diendorfer, Influence of channel base current and varying return stroke speed on the calculated fields of three important return stroke models, paper presented at International Conference on Lightning and Static Electricity, Cocoa Beach, Fl., NASA Conf. Publ. 3106, 1991.

Thottappillil, R., V. A. Rakov, and M. A. Uman, Distribution of charge along the lightning channel: Relation to remote electric and magnetic fields and to return-stroke models, *J. Geophys. Res.*, *102*, 6987-7006, 1997.

Uman, M.A., and D. K. McLain, Magnetic field of lightning return stroke, *J. Geophys. Res.*, *74*, 6899-6910, 1969.

Rouzbeh Moini, Electrical Engineering Department, Amirkabir University of Technology, Tehran 15914, Iran. (moini@cic.aku.ac.ir)

Behzad Kordi, Electrical Engineering Department, Faculty of Engineering, Bahonar University, Kerman, Iran. (behzad.kordi@ieee.org)

Gholamreza Z. Rafi, Electrical Engineering Department, Zanjan University, Zanjan, Iran. (ghrafi@mail.znu.ac.ir)

Vladimir A. Rakov, Department of Electrical and Computer Engineering, University of Florida, Gainesville, FL 32611. (rakov@ece.ufl.edu)

(Received March 1, 2000; revised August 8, 2000; accepted August 22, 2000.)